

Measurement-Induced Collective Vibrational Quantum Coherence under Spontaneous Raman Scattering in a Liquid

Valeria Vento[†], Santiago Tarrago Velez[†], Anna Pogrebna, and Christophe Galland^{*}

*École polytechnique fédérale de Lausanne (EPFL),
Institute of Physics, CH-1015 Lausanne, Switzerland* [†]

(Dated: May 17, 2022)

Spontaneous vibrational Raman scattering is a ubiquitous form of light-matter interaction whose description necessitates quantization of the electromagnetic field. It is usually considered as an incoherent process because the scattered field lacks any predictable phase relationship with the incoming field. When probing an ensemble of molecules, the question therefore arises: What quantum state should be used to describe the molecular ensemble following spontaneous Stokes scattering? In this Letter, we experimentally address this question by measuring time-resolved Stokes–anti-Stokes two-photon coincidences on a molecular liquid consisting of several sub-ensembles with slightly different vibrational frequencies. When spontaneously scattered Stokes photons and subsequent anti-Stokes photons are detected into a single spatiotemporal mode, the observed dynamics is inconsistent with a statistical mixture of individually excited molecules. Instead, we show that the data are reproduced if Stokes–anti-Stokes correlations are mediated by a collective vibrational quantum, i.e. a coherent superposition of all molecules interacting with light. Our results demonstrate that the degree of coherence in the vibrational state of the liquid is not an intrinsic property of the material system, but rather depends on the optical excitation and detection geometry.

Introduction.— Raman scattering was first reported in 1928 [1] and with the advent of laser sources it has become an essential tool for probing and understanding the vibrational structure of organic and inorganic matter. In a majority of experiments, a semi-classical model of light-matter interaction is sufficient to interpret the results of Raman spectroscopy. For example, the intensity asymmetry between Stokes and anti-Stokes scattering is obtained by quantizing the vibrational modes of each individual molecule. A full quantum theory of Raman scattering was developed in the 70’s and 80’s [2–7], and its predictions were tested, e.g., by measuring intensity fluctuations in stimulated Raman scattering [8–10].

Following a pioneering work by Walmsley and coworkers in 2011 [11], more recent experiments have used time-correlated single photon counting to evidence non-classical intensity correlations between light fields interacting with the same phonon mode via Raman scattering, with potential applications in ultrafast quantum information processing [12–17], novel forms of spectroscopy [18, 19], and the generation of non-classical states of light [20]. These experimental results have spurred further theoretical developments to understand how the Raman process leads to photonic correlations mediated by a phononic excitation [21–24], how the experimental geometry impacts the photon statistics of the Stokes field [25], and how the coupling of a Raman-active mode to a nanocavity modifies the dynamics of the system [26–28].

To our knowledge, and despite this recent experimental progress, there has been no direct measurement of the nature of the vibrational quantum state generated in an ensemble of molecules in the liquid phase. Since

molecule-molecule interactions in a liquid are in general incoherent and only contribute to vibrational relaxation [29], they cannot generate spatial coherence over mesoscopic length scales – in contrast to crystalline materials, in which near-field Raman scattering experiments [30–32] have deduced phonon coherence lengths on the order of tens of nanometers. Accordingly, most reference texts assume that coherence among different molecules can only be imposed by external driving, e.g. with the beat note between two strong laser fields as in Coherent anti-Stokes Raman scattering (CARS) [33]. Quantum coherence among different molecules following spontaneous Raman scattering in a dense molecular liquid has often been neglected [34, 35], implicitly assuming that the resulting collective vibrational state is a statistical mixture of individually excited molecules. We note that when studying an ensemble of identical molecules, the temporal coherence of the Stokes field [19, 36] or the presence of Stokes–anti-Stokes coincidences [37, 38] do not provide direct information about the collective coherence possibly existing among the molecules – which is why the authors from Ref. [38] could describe their experiment in terms of single-molecule scattering events.

In this Letter, we demonstrate that spontaneous vibrational Raman scattering in the liquid phase and at room temperature can also induce a collective vibrational state, i.e. a quantum superposition of a macroscopic number of individually excited molecules. To this end, we use a liquid of carbon disulfide (CS₂) that naturally contains a few distinct molecular sub-ensembles defined by the initial vibrational state and isotope content of each molecule and having slightly different vibration frequencies (Fig. 1). We measure time-resolved two-photon Stokes–anti-Stokes correlations mediated by the creation and annihilation of a vibrational quantum in the

^{*} chris.galland@epfl.ch

[†] These authors contributed equally to this work

symmetric stretch mode of the molecules, and observe revivals after several picoseconds. These quantum beats are signatures of a coherent superposition where a single vibrational quantum is shared between all molecules involved in Raman scattering and belonging to a spatial mode selected by the measurement geometry. Our results are consistent with the numerous works on emissive quantum memories using atomic ensembles [39] where collective quantum coherence can be induced by post-selection upon single photon detection – a key concept underlying the DLCZ proposal for quantum repeaters [40]. As proposed in the context of cavity optomechanics [41], our data are also consistent with the emergence of mode entanglement between molecular sub-ensembles upon single photon detection.

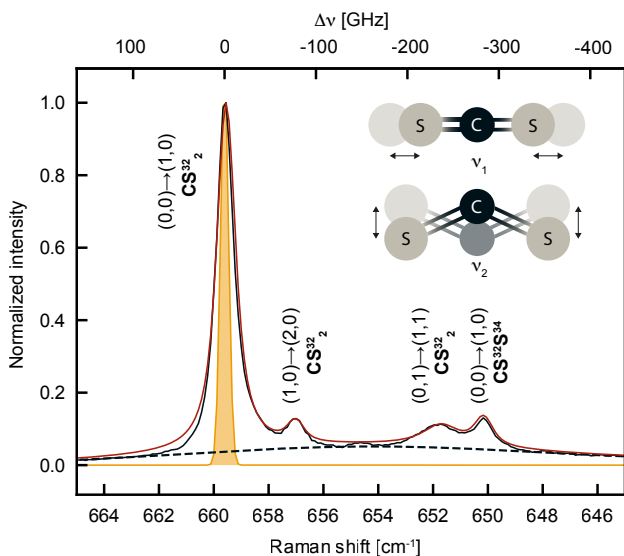


FIG. 1. Continuous-wave Raman spectrum of liquid CS_2 . The black solid line represents the normalized Stokes intensity measured under 780 nm laser excitation. Each peak is associated with a molecular transition of a particular CS_2 isotope. In the notation $(n_1^{init.}, n_2^{init.}) \rightarrow (n_1^{fin.}, n_2^{fin.})$, n_1 and n_2 are the quantum numbers of the symmetric stretching mode $\nu_1(\Sigma_g^+)$ and the two-fold degenerate bending mode $\nu_2(\Pi_u)$, respectively, as sketched in the inset. After subtracting the background (dashed line), the spectrum has been fitted in frequency space with the sum of four Voigt functions (red line) with fixed Gaussian contribution (orange profile) as described in the text.

Sample characterization.— Fig.1 shows the Raman spectrum of CS_2 liquid (anhydrous, $\geq 99\%$, Sigma Aldrich) at room temperature, focusing on the symmetric stretch mode ν_1 , acquired under 780 nm continuous-wave excitation with a high-resolution Shamrock SR-750 spectrometer equipped with a Newton 940 camera (Andor) and a 1800 l/mm 400 nm blaze grating. Note that CS_2 has no electronic transition at visible or near-infrared frequencies so that all measurements reported here correspond to far off-resonance excitation. The vibrational

transitions associated to the four main peaks in Fig.1 are assigned following Refs. [42–44], and are labelled according the initial (at thermal equilibrium) and final (after Stokes scattering) occupation numbers of the stretching (ν_1) and bending (ν_2) vibrational modes.

We recognize the pure ν_1 bands of the two dominant isotopes CS_2^{32} and $\text{CS}_2^{32}\text{S}^{34}$ at 659.6 cm^{-1} and 650.1 cm^{-1} , respectively, and two hot bands of CS_2^{32} at 657 cm^{-1} and 651.7 cm^{-1} . In the following, these four dominant vibrational transitions are simply labeled with $i = 1, 2, 3, 4$ in order of decreasing Raman shift. The pure ν_1 band of $\text{CS}_2^{32}\text{S}^{33}$ (barely distinguishable around 655 cm^{-1}) and other hot bands of the three isotopes CS_2^{32} , $\text{CS}_2^{32}\text{S}^{33}$ and $\text{CS}_2^{32}\text{S}^{34}$ contribute to the background used in our fit and marked as dashed lines.

After background subtraction we fitted the Raman spectrum in frequency space with the sum of four Voigt functions: for each peak, we assume that the Raman line shape is Lorentzian, while the Gaussian contribution is fixed by the instrument response function. The latter is estimated by measuring the spectrum of the attenuated excitation laser, which is well fit with a Gaussian of $\sim 0.02\text{ nm}$ FWHM (orange shaded peak), in agreement with the nominal system resolution. The free fit parameters are the central frequencies of the four Raman peaks and the FWHMs $\Delta\nu_i$ of three modes ($i = 1, 2, 3$) – the pure ν_1 vibrations of both isotopes are supposed to have the same linewidth, $\Delta\nu_1 = \Delta\nu_4$. The relative intensities among all peaks are fixed by temperature and isotope abundance following Ref. [42]. From the Raman shifts, we obtain the four vibrational frequencies: 20.04, 19.96, 19.81 and 19.76 THz. From the Lorentzian width, we infer the effective coherence time $T_2 = (\pi\Delta\nu)^{-1}$ of each vibration in our measurement geometry: 15.71, 18.38, 6.77 and 15.71 ps respectively.

Experimental Results.— We use the technique introduced in [45]; simplified description of the experimental setup is provided in Fig.2. A first near-infrared laser pulse ($\sim 200\text{ fs}$ pulse duration, 80 MHz repetition rate) generates a two-mode photon-phonon squeezed state via spontaneous Stokes scattering. The power is adjusted to generate less than 10^{-2} Stokes photon per pulse within the spatial mode selected by the collection fiber, far below the onset of any stimulated Raman process. After this *write* pulse, a *read* pulse centered at a different wavelength is used to probe the vibrational mode occupancy after a variable time delay t . This information is encoded in the Stokes–anti-Stokes correlation function $g_{S,A}^{(2)}(t)$ [46, 47]. In the limit of low scattering probability and absent any background emission nor noise, the strength of vibration-mediated correlation is upper-bounded by $g_{S,A}^{(2)} < 1 + 1/n_{th} \simeq 26$, where the thermal occupancy of the vibrational mode is $n_{th} \simeq 0.04$ in our system at room-temperature.

The sample is studied in transmission to fulfill momentum conservation in the Stokes – anti-Stokes process mediated by a collective vibration with van-

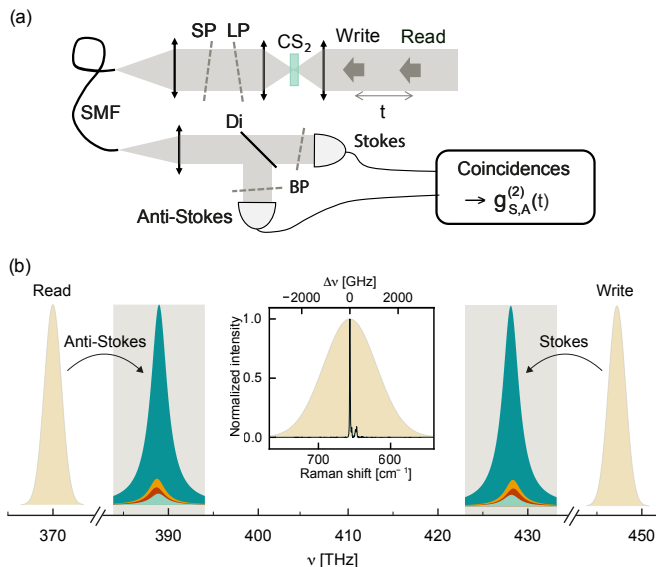


FIG. 2. (a) Sketch of the experimental setup. Liquid CS₂ is held between two objective lenses (numerical aperture: 0.8) in a quartz cuvette sealed with parafilm with ~ 0.2 mm wall thickness and ~ 1 mm optical path. Fiber-coupled single photon avalanche photodiodes are connected to a coincidence counter to measure $g_{S,A}^{(2)}$. SP: shortpass; LP: longpass; BP: bandpass; Di: dichroic; SMF: single mode fiber. (b) Frequency-domain schematic of experimentally relevant optical fields. Only the Stokes signal from the write pulse and the anti-Stokes signal from the read pulse are transmitted through the filters to their respective detectors (grey area). Each Raman peak is broadened to the linewidth of the excitation pulse (~ 200 fs duration) so that adjacent vibrational modes (Fig.1) are no longer distinguishable. A comparison between the excitation pulses and the continuous-wave Raman spectrum is shown in the inset.

ishing momentum. The Raman signal is collected into a single mode optical fiber whose back-propagated image overlaps with the focused laser beams to define a single spatial mode inside the sample. After spatial filtering through the fiber, the Stokes and anti-Stokes photons from the first and second pulses, respectively, are separated based on their non-overlapping spectra and individually detected.

Figure 3 shows $g_{S,A}^{(2)}(t)$ plotted as a function of time delay between Stokes and anti-Stokes processes. When write and read pulses temporally overlap, virtual electronic processes contribute to four-wave mixing (FWM) and generate photon pairs at any frequencies satisfying energy conservation (phase matching is highly relaxed in our strongly focused geometry), causing a strong rise in $g_{S,A}^{(2)}$. We used crossed-polarised laser pulses to minimize the relative contribution of electronic FWM to the overall signal.

Beyond $t \simeq 1$ ps, instantaneous contributions to FWM have vanished and $g_{S,A}^{(2)}(t) > 1$ is a signature of intensity correlations between Stokes and anti-Stokes fields medi-

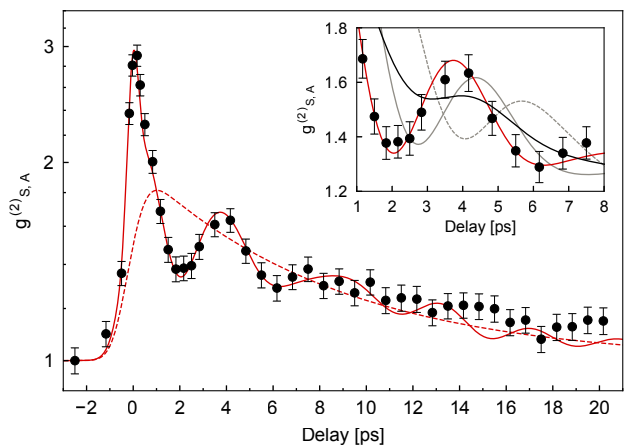


FIG. 3. Write-read delay dependence of the measured normalised Stokes–anti-Stokes correlations (full circles) and model prediction (solid red line). Only Raman photons co-polarised with their respective laser pulses were selected. Free fitting parameters entering the model curve are a scaling amplitude $A_{tot} = 1.79$, and the relative phases (in radian) are $\theta_2 = 2.67$; $\theta_3 = 0.06$ and $\theta_4 = -0.4$. The dotted red line represents the multi-exponential decay that would result from a statistical mixture of single vibrating molecules. Inset: model predictions for different values of the phases: in particular by adding a phase of $\pi/6$ (grey solid line) and $\pi/2$ (grey dashed line) to each θ_i . The black line in the inset is the sum of the three curves showing reduced visibility of oscillations.

ated by molecular vibrations. The red dashed curve is a tentative fit with a multi-exponential decay whose relative amplitudes and time constants are extracted from Fig. 1. This decay would result from describing the vibrational state as a statistical mixture with one molecule excited at random for each coincidence count. While this model matches the overall damping of correlations, it fails to capture the clear oscillations in the value of $g_{S,A}^{(2)}(t)$.

We note that oscillations resulting from the excitation of vibrational modes in different isotopes of CCl₄ [48] were observed using ultrafast stimulated Raman scattering in Ref. [49, 50]. However such experiments are well accounted for by a semi-classical model, in which the stimulated Stokes and anti-Stokes fields are classical. In the case of stimulated Raman scattering, the beating between the two pump laser fields is tuned resonant with the molecular vibration of interest, thereby driving a coherent collective vibration and resulting in a coherently oscillating Raman polarisation in the sample, all of which behave as classical variables.

In contrast, spontaneous Raman scattering and single photon counting demand a quantum description, in which the post-selected vibrational state naturally appears as a quantum coherent superposition involving all molecules coupled to the light field. Such a quantum model is detailed in the Supplementary Material and solved numerically; here we prefer to present instead a simplified analytical model that does reproduce the

observed quantum beats.

We assume that each collective vibrational mode (which correspond to the four distinct subsets of molecules) contribute to the Stokes–anti-Stokes correlations with a complex amplitude

$$\lambda_i(t) = a_i e^{-t/T_{2,i}} e^{-i\theta_i - i\Omega_i t} \quad (1)$$

for $i=1,2,3,4$, where $a_i \simeq [0.70, 0.03, 0.21, 0.06]$ correspond to the fractional contributions to the intensity as extracted from Ref. [42], Ω_i and $T_{2,i}$ are the phonon frequency in rad/s and the coherence times extracted from the spectrum in Fig. 1, and θ_i are phase offsets. Since only phase differences between modes are measurable, we set $\theta_1 = 0$.

The total signal features interference between these terms,

$$g_{\text{model}}^{(2)}(t) - 1 = A_{\text{tot}} \left| \sum_i \lambda_i(t) \right|^2. \quad (2)$$

We used this model to fit the oscillations with only the total amplitude A_{tot} and the three relative phases θ_i as free parameters. The complete fit function has the following expression:

$$F_{\text{model}} = g_{\text{model}}^{(2)} * f_{\text{rise}} + G_{\text{FWM}}. \quad (3)$$

where we convolute with a rise function and add a Gaussian function centered at zero delay that accounts for electronic FWM.

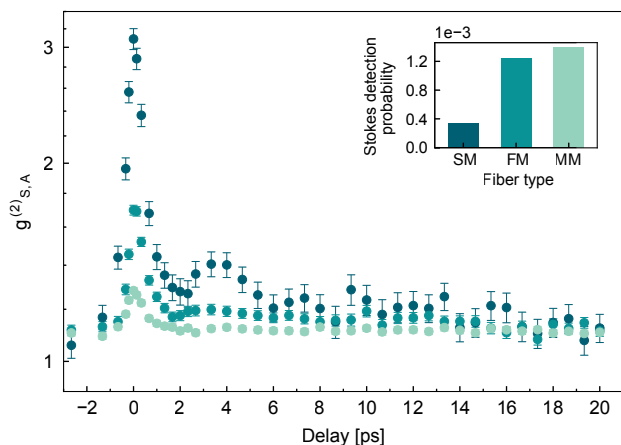


FIG. 4. Measured $g_{S,A}^{(2)}(t)$ using different optical fibers in collection path (see Fig. 2a). From darker to lighter color: 3.5- μm core single-mode fiber (SM), 9- μm core telecom fiber (FM, few-mode), and 50- μm core multimode (MM) fiber. In the inset, we show the Stokes detection probability for the different fibers.

While the quality of the fit provides strong support for our model, similar quantum beats would also result from

coherence between energy levels of a single molecule. In such a case, the exact detection geometry would have no impact on the observations, and in particular it would not be essential to post-select a single spatial mode to observe quantum beats.

To test this hypothesis we repeat the same measurement using increasing fiber core sizes in the collection path, and therefore increasing number of spatial modes contributing to the total signal, with results shown in Fig. 4. The loss of visibility when measuring multiple optical modes provides further evidence that the observations are due to the spatial coherence generated through the experimental geometry and measurement post-selection.

Conclusions.— To summarize, we presented a time domain measurement of spectrally resolved Stokes–anti-Stokes two-photon correlations on liquid CS_2 at room temperature, in the regime of spontaneous Raman scattering (Stokes scattering probability $\sim 1\%$). Upon post-selection of events where both Stokes and anti-Stokes photons are collected through the same single-mode optical fiber, we observe quantum beats that are perfectly consistent with a macroscopic quantum superposition of molecules sharing a single quantum of vibration. In particular, our experimental results are incompatible with the picture according to which spontaneous Raman scattering from a large ensemble is always the incoherent sum (statistical mixture) of single-molecule scattering events.

Our experiment nourishes the debate about the relation between optical coherence and quantum coherence [51, 52] and entanglement [53]. It questions whether optical coherent states are necessary to explain various forms of coherent Raman spectroscopy, for we do not stimulate the Raman process and yet observe coherent oscillations, as if we did.

In the future, our photon counting approach can be adapted to probe inter- or intramolecular vibrational entanglement in more complex systems, as well as excitonic and vibrational polariton dynamics [54]. We also envision extensions of our work to probe how Raman scattering is affected by collective excitonic [55–58] or vibrational [59–64] strong coupling to a cavity, with implications for polariton chemistry [65].

ACKNOWLEDGEMENTS

The authors thank Vivishek Sudhir for insightful discussions and valuable comments. This work has received funding from the Swiss National Science Foundation (SNSF) (projects no. 170684 and 198898) and the European Research Council’s (ERC) Horizon 2020 research and innovation programme (grant agreement no. 820196) A. P. acknowledges funding from the European Union’s Horizon 2020 research and innovation programme under the Marie Skłodowska-Curie grant agreement N° 754462.

-
- [1] C. V. Raman and K. S. Krishnan, A new type of secondary radiation, *Nature* **121**, 501 (1928).
- [2] D. F. Walls, Quantum theory of the Raman effect, *Zeitschrift für Physik A Hadrons and nuclei* **237**, 224 (1970).
- [3] D. F. Walls, Quantum theory of the raman effect, *Zeitschrift für Physik A Hadrons and nuclei* **244**, 117 (1971).
- [4] T. von Foerster and R. J. Glauber, Quantum theory of light propagation in amplifying media, *Phys. Rev. A* **3**, 1484 (1971).
- [5] J. Mostowski and M. Raymer, The buildup of stimulated Raman scattering from spontaneous Raman scattering, *Optics Communications* **36**, 237 (1981).
- [6] M. G. Raymer and J. Mostowski, Stimulated raman scattering: Unified treatment of spontaneous initiation and spatial propagation, *Phys. Rev. A* **24**, 1980 (1981).
- [7] M. G. Raymer, I. A. Walmsley, J. Mostowski, and B. Sobolewska, Quantum theory of spatial and temporal coherence properties of stimulated raman scattering, *Phys. Rev. A* **32**, 332 (1985).
- [8] I. A. Walmsley and M. G. Raymer, Observation of macroscopic quantum fluctuations in stimulated raman scattering, *Phys. Rev. Lett.* **50**, 962 (1983).
- [9] I. A. Walmsley and M. G. Raymer, Experimental study of the macroscopic quantum fluctuations of partially coherent stimulated raman scattering, *Phys. Rev. A* **33**, 382 (1986).
- [10] M. G. Raymer, Z. W. Li, and I. A. Walmsley, Temporal quantum fluctuations in stimulated raman scattering: Coherent-modes description, *Phys. Rev. Lett.* **63**, 1586 (1989).
- [11] K. C. Lee, M. R. Sprague, B. J. Sussman, J. Nunn, N. K. Langford, X.-M. Jin, T. Champion, P. Michelberger, K. F. Reim, D. England, D. Jaksch, and I. A. Walmsley, Entangling Macroscopic Diamonds at Room Temperature, *Science* **334**, 1253 (2011).
- [12] K. C. Lee, B. J. Sussman, M. R. Sprague, P. Michelberger, K. F. Reim, J. Nunn, N. K. Langford, P. J. Bustard, D. Jaksch, and I. A. Walmsley, Macroscopic non-classical states and terahertz quantum processing in room-temperature diamond, *Nature Photonics* **6**, 41 (2012).
- [13] D. G. England, P. J. Bustard, J. Nunn, R. Lausten, and B. J. Sussman, From Photons to Phonons and Back: A THz Optical Memory in Diamond, *Phys. Rev. Lett.* **111**, 243601 (2013).
- [14] D. G. England, K. Fisher, J.-P. W. MacLean, P. J. Bustard, R. Lausten, K. J. Resch, and B. J. Sussman, Storage and Retrieval of THz-Bandwidth Single Photons Using a Room-Temperature Diamond Quantum Memory, *Phys. Rev. Lett.* **114**, 053602 (2015).
- [15] P.-Y. Hou, Y.-Y. Huang, X.-X. Yuan, X.-Y. Chang, C. Zu, L. He, and L.-M. Duan, Quantum teleportation from light beams to vibrational states of a macroscopic diamond, *Nat. Commun.* **7**, 11736 (2016).
- [16] K. A. Fisher, D. G. England, J. P. W. MacLean, P. J. Bustard, K. J. Resch, and B. J. Sussman, Frequency and bandwidth conversion of single photons in a room-temperature diamond quantum memory, *Nature Communications* **7**, 5 (2016).
- [17] K. A. G. Fisher, D. G. England, J.-P. W. MacLean, P. J. Bustard, K. Heshami, K. J. Resch, and B. J. Sussman, Storage of polarization-entangled THz-bandwidth photons in a diamond quantum memory, *Phys. Rev. A* **96**, 012324 (2017).
- [18] F. C. Waldermann, B. J. Sussman, J. Nunn, V. O. Lorenz, K. C. Lee, K. Surmacz, K. H. Lee, D. Jaksch, I. A. Walmsley, P. Spizziri, P. Olivero, and S. Prawer, Measuring phonon dephasing with ultrafast pulses using Raman spectral interference, *Physical Review B* **78**, 155201 (2008).
- [19] S. Meiselman, O. Cohen, M. F. DeCamp, and V. O. Lorenz, Observation of coherence oscillations of single ensemble excitations in methanol, *Journal of the Optical Society of America B* **31**, 2131 (2014).
- [20] S. T. Velez, V. Sudhir, N. Sangouard, and C. Galland, Bell correlations between light and vibration at ambient conditions, *Science Advances* **6**, eabb0260 (2020).
- [21] A. Saraiva, F. S. d. A. Júnior, R. de Melo e Souza, A. P. Pena, C. H. Monken, M. F. Santos, B. Koiller, and A. Jorio, Photonic counterparts of cooper pairs, *Phys. Rev. Lett.* **119**, 193603 (2017).
- [22] C. A. Parra-Murillo, M. F. Santos, C. H. Monken, and A. Jorio, Stokes-anti-stokes correlation in the inelastic scattering of light by matter and generalization of the bose-einstein population function, *Phys. Rev. B* **93**, 125141 (2016).
- [23] K. Thapliyal and J. Peřina Jr, Ideal pairing of the stokes and anti-stokes photons in the raman process, *Physical Review A* **103**, 033708 (2021).
- [24] R. A. Diaz, C. Monken, A. Jorio, and M. F. Santos, Effective hamiltonian for stokes-anti-stokes pair generation with pump and probe polarized modes, *Physical Review B* **102**, 134304 (2020).
- [25] K. Shinbrough, Y. Teng, B. Fang, V. O. Lorenz, and O. Cohen, Photon-matter quantum correlations in spontaneous raman scattering, *Physical Review A* **101**, 013415 (2020).
- [26] P. Roelli, C. Galland, N. Piro, and T. J. Kippenberg, Molecular cavity optomechanics as a theory of plasmon-enhanced Raman scattering, *Nat Nano* **11**, 164 (2016).
- [27] Y. Zhang, J. Aizpurua, and R. Esteban, Optomechanical collective effects in surface-enhanced raman scattering from many molecules, *ACS Photonics* **7**, 1676 (2020), <https://doi.org/10.1021/acsp Photonics.0c00032>.
- [28] M. K. Schmidt, R. Esteban, G. Giedke, J. Aizpurua, and A. Gonzalez-Tudela, Frequency-resolved photon correlations in cavity optomechanics, *Quantum Science and Technology* (2021).
- [29] D. W. Oxtoby, Vibrational relaxation in liquids, *Annual Review of Physical Chemistry* **32**, 77 (1981), <https://doi.org/10.1146/annurev.pc.32.100181.000453>.
- [30] R. Beams, L. G. Cancado, S.-H. Oh, A. Jorio, and L. Novotny, Spatial coherence in near-field raman scattering, *Phys. Rev. Lett.* **113**, 186101 (2014).
- [31] L. G. Cancado, R. Beams, A. Jorio, and L. Novotny, Theory of spatial coherence in near-field raman scattering, *Phys. Rev. X* **4**, 031054 (2014).
- [32] R. S. Alencar, C. Rabelo, H. L. S. Miranda, T. L. Vasconcelos, B. S. Oliveira, A. Ribeiro, B. C. Púbbio, J. Ribeiro-Soares, A. G. S. Filho, L. G.

- Cançado, and A. Jorio, Probing spatial phonon correlation length in post-transition metal monochalcogenide gas using tip-enhanced raman spectroscopy, *Nano Letters* **19**, 7357 (2019), pMID: 31469281, <https://doi.org/10.1021/acs.nanolett.9b02974>.
- [33] B. Schrader, *Infrared and Raman spectroscopy: methods and applications* (John Wiley & Sons, 2008).
- [34] D. A. Long, *The Raman effect: a unified treatment of the theory of Raman scattering by molecules* (Wiley, 2002).
- [35] E. Le Ru and P. Etchegoin, *Principles of Surface-Enhanced Raman Spectroscopy: and related plasmonic effects* (Elsevier, 2008).
- [36] L. Sun, P. Kumar, Z. Liu, J. Choi, B. Fang, S. Roesch, K. Tran, J. Casara, E. Priego, Y.-M. Chang, G. Moody, K. L. Silverman, V. O. Lorenz, M. Scheibner, T. Luo, and X. Li, Phonon dephasing dynamics in mos₂, *Nano Letters* **21**, 1434 (2021), pMID: 33508204, <https://doi.org/10.1021/acs.nanolett.0c04368>.
- [37] P. J. Bustard, J. Erskine, D. G. England, J. Nunn, P. Hockett, R. Lausten, M. Spanner, and B. J. Sussman, Nonclassical correlations between terahertz-bandwidth photons mediated by rotational quanta in hydrogen molecules, *Opt. Lett.*, OL **40**, 922 (2015).
- [38] M. Kasperczyk, F. S. De Aguiar Júnior, C. Rabelo, A. Saraiva, M. F. Santos, L. Novotny, and A. Jorio, Temporal Quantum Correlations in Inelastic Light Scattering from Water, *Physical Review Letters* **117**, 1 (2016).
- [39] F. Bussieres, N. Sangouard, M. Afzelius, H. De Riedmatten, C. Simon, and W. Tittel, Prospective applications of optical quantum memories, *Journal of Modern Optics* **60**, 1519 (2013).
- [40] L.-M. Duan, M. D. Lukin, J. I. Cirac, and P. Zoller, Long-distance quantum communication with atomic ensembles and linear optics, *Nature* **414**, 413 (2001).
- [41] H. Flayac and V. Savona, Heralded preparation and readout of entangled phonons in a photonic crystal cavity, *Physical Review Letters* **113**, 1 (2014), arXiv:1407.5275.
- [42] T. Cox, M. Battaglia, and P. Madden, Properties of liquid CS₂ from the allowed light scattering spectra, *Molecular Physics* **38**, 1539 (1979).
- [43] B. P. Stoicheff, High resolution Raman spectroscopy of gases: XI. Spectra of CS₂ and CO₂, *Can. J. Phys.* **36**, 218 (1958), tex.ids= stoicheff_high_1958 tex.bdsck-url-2: <https://doi.org/10.1139/p58-026>.
- [44] E. K. Plyler and C. J. Humphreys, Infrared absorption spectrum of carbon disulfide, *Journal of Research of the National Bureau of Standards* **39**, 59 (1947).
- [45] M. D. Anderson, S. Tarrago Velez, K. Seibold, H. Flayac, V. Savona, N. Sangouard, and C. Galland, Two-Color Pump-Probe Measurement of Photonic Quantum Correlations Mediated by a Single Phonon, *Physical Review Letters* **120**, 233601 (2018).
- [46] C. Galland, N. Sangouard, N. Piro, N. Gisin, and T. J. Kippenberg, Heralded single-phonon preparation, storage, and readout in cavity optomechanics, *Phys. Rev. Lett.* **112**, 143602 (2014).
- [47] R. Riedinger, S. Hong, R. A. Norte, J. A. Slater, J. Shang, A. G. Krause, V. Anant, M. Aspelmeyer, and S. Gröblacher, Non-classical correlations between single photons and phonons from a mechanical oscillator, *Nature* **530**, 313 (2016).
- [48] C. K. Wu and G. B. B. M. Sutherland, The Isotope Effect in the Vibration Spectrum of CCl₄, *The Journal of Chemical Physics* **6**, 114 (1938).
- [49] A. Laubereau, G. Wochner, and W. Kaiser, Collective beating of molecular vibrations in liquids on the picosecond time scale, *Optics Communications* **17**, 91 (1976).
- [50] J. Konarska, W. Gadomski, B. Ratajska-Gadomska, K. Polok, G. Pudłowski, and T. M. Kardaś, Dynamics of intermolecular interactions in CCl₄ via the isotope effect by femtosecond time-resolved spectroscopy, *Physical Chemistry Chemical Physics* **18**, 16046 (2016).
- [51] K. Mølmer, Optical coherence: A convenient fiction, *Physical Review A* **55**, 3195 (1997).
- [52] S. D. BARTLETT, T. RUDOLPH, and R. W. SPEKKENS, Dialogue concerning two views on quantum coherence: Factist and fictionist, *International Journal of Quantum Information* **04**, 17 (2006), <https://doi.org/10.1142/S0219749906001591>.
- [53] A. Karnieli, N. Rivera, A. Arie, and I. Kaminer, The coherence of light is fundamentally tied to the quantum coherence of the emitting particle, *Science Advances* **7**, 10.1126/sciadv.abf8096 (2021).
- [54] K. E. Dorfman and S. Mukamel, Multidimensional photon correlation spectroscopy of cavity polaritons, *Proceedings of the National Academy of Sciences* **115**, 1451 (2018), <https://www.pnas.org/content/115/7/1451.full.pdf>.
- [55] J. Galego, F. J. Garcia-Vidal, and J. Feist, Cavity-induced modifications of molecular structure in the strong-coupling regime, *Phys. Rev. X* **5**, 041022 (2015).
- [56] F. C. Spano, Optical microcavities enhance the exciton coherence length and eliminate vibronic coupling in j-aggregates, *The Journal of Chemical Physics* **142**, 184707 (2015), <https://doi.org/10.1063/1.4919348>.
- [57] F. Herrera and F. C. Spano, Cavity-controlled chemistry in molecular ensembles, *Phys. Rev. Lett.* **116**, 238301 (2016).
- [58] A. G. Avramenko and A. S. Rury, Interrogating the structure of molecular cavity polaritons with resonance raman scattering: An experimentally motivated theoretical description, *The Journal of Physical Chemistry C* **123**, 30551 (2019), <https://doi.org/10.1021/acs.jpcc.9b08716>.
- [59] A. Shalabney, J. George, H. Hiura, J. A. Hutchison, C. Genet, P. Hellwig, and T. W. Ebbesen, Enhanced raman scattering from vibro-polariton hybrid states, *Angewandte Chemie International Edition* **54**, 7971 (2015), <https://onlinelibrary.wiley.com/doi/pdf/10.1002/anie.201502979>.
- [60] J. del Pino, J. Feist, and F. J. Garcia-Vidal, Signatures of vibrational strong coupling in raman scattering, *The Journal of Physical Chemistry C* **119**, 29132 (2015), <https://doi.org/10.1021/acs.jpcc.5b11654>.
- [61] J. del Pino, F. J. Garcia-Vidal, and J. Feist, Exploiting vibrational strong coupling to make an optical parametric oscillator out of a raman laser, *Phys. Rev. Lett.* **117**, 277401 (2016).
- [62] A. Strashko and J. Keeling, Raman scattering with strongly coupled vibron-polaritons, *Phys. Rev. A* **94**, 023843 (2016).
- [63] P. Roelli, D. Martin-Cano, T. J. Kippenberg, and C. Galland, Molecular platform for frequency upconversion at the single-photon level, *Phys. Rev. X* **10**, 031057 (2020).
- [64] S. Hughes, A. Settineri, S. Savasta, and F. Nori, Resonant raman scattering of single molecules under simultaneous strong cavity coupling and ultrastrong optomechanical coupling: phonon-dressed polaritons, arXiv , 2103.08670 (2021).

- [65] R. F. Ribeiro, L. A. Martínez-Martínez, M. Du, J. Campos-Gonzalez-Angulo, and J. Yuen-Zhou, Polariton chemistry: controlling molecular dynamics with optical cavities, *Chem. Sci.* **9**, 6325 (2018).